An extended MSPAC method in circular arrays

Elham Shabani, Pierre-Yves Bard, Noorbakhsh Mirzaei, Morteza Eskandari-Ghadi, Cecile Cornou, Ebrahim Haghshenas

Geophysical Journal International

Geophys. J. Int. (2010) **182,** 1431–1437 doi: 10.1111/j.1365-246X.2010.04687.x

An extended MSPAC method in circular arrays

Elham Shabani,[1] Pierre-Yves Bard,[2] Noorbakhsh Mirzaei,[1] Morteza Eskandari-Ghadi,[3] Cecile Cornou[2] and Ebrahim Haghshenas[4]

[1]*Institute of Geophysics, University of Tehran, Iran. E-mail: eshabani@ut.ac.ir*
[2]*Laboratoire de Géophysique Interne et Tectonophysique, Université J. Fourier, Maison des Géosciences, Grenoble, France*
[3]*Department of Engineering Science, University of Tehran, Iran*
[4]*International Institute of Earthquake Engineering and Seismology, Tehran, Iran*

Accepted 2010 May 31. Received 2010 May 26; in original form 2008 December 7

SUMMARY

The microtremor seismic method using spatial autocorrelation (SPAC) processing is a useful tool for estimating the structure of subsurface layers and the shear wave velocities of sediments. This paper improves upon the well-known 'Modified SPAC' (MSPAC) method, which extends the SPAC formulae for discrete and nearly continuous circular arrays to handle arrays with regular and irregular azimuthal spacing. For finite circular arrays, extended MSPAC (EMSPAC) also takes into account the discrete character of the array, which has been inspired by the works of Okada. Also a new SPAC coefficient is proposed for a nearly continuous array. EMSPAC is applied to real data collected using a seven-station array, and its averaged SPAC coefficients and dispersion curves are compared to those obtained using MSPAC.

Key words: Spatial analysis; Surface waves and free oscillations; Site effects.

GJI Seismology

1 INTRODUCTION

Array measurements of seismic microtremors or ambient noise are currently employed as an easy and low-cost procedure for soil profiling (e.g. Okada 2003; Apostolidis *et al.* 2004; Morikawa *et al.* 2004). These methods determine the physical properties and structure of the crust by timing the propagation of natural vibrations. Furthermore, array measurements are less expensive than invasive methods such as boreholes and standard penetration tests (SPT) (García-Jerez *et al.* 2008).

The two most popular microtremor processing techniques are frequency–wavenumber (*F–K*, Capon 1969; Lacoss *et al.* 1969) and spatial autocorrelation (SPAC, Aki 1957; Asten 1976). The SPAC method, which generally employs a circular array of stations and one central station, permits an in-depth understanding of the temporal and spatial spectra of seismic waves. Nowadays, it is widely used to estimate the structure of subsurface layers and the shear wave velocities of sediments (Okada *et al.* 1990; Matsuoka *et al.* 1996; Kudo *et al.* 2002; Okada 2003). In the SPAC method, the dispersion curves (phase velocity versus frequency) of surface waves are deduced by analysing the normalized correlations between microtremors recorded at different stations. The dispersion curves are then used to characterize the structure of the medium. The method is based on a statistical analysis of the observed signal, which is assumed to be stationary and ergodic in time and space (see Bettig *et al.* 2001).

The original mathematical model proposed by Aki (1957) and Asten (1976) posits an infinite number of stations along the circumference of a circle, and one station in the centre. Many subsequent studies are based on their fundamental theory (e.g. Okada *et al.* 1990; Matsuoka *et al.* 1996; Kudo *et al.* 2002; Okada 2003), but use a finite number of stations. In addition, some authors have modified and extended the traditional SPAC technique. Bettig *et al.* (2001) revised the SPAC technique to deal with irregular arrays, naming the result modified spatial autocorrelation (MSPAC). They paid special attention to the distribution of station azimuths while considering the correlations between each pair of received signals in the circumferential stations. Ohori *et al.* (2002) introduced a SPAC procedure suitable for more complex arrays, which employs higher modes of the Rayleigh waves. In more recent works, both Cho *et al.* (2006) and García-Jerez *et al.* (2006, 2008) have proposed similar methods for calculating Rayleigh- and Love-wave dispersion curves based on the horizontal components of microtremors recorded by a double circular array. Chávez-García *et al.* (2005) showed that averaging the correlation of a single station pair over many time windows is equivalent to azimuthal averaging over a circular array (see also Morikawa *et al.* 2004; Chávez-García & Luzón 2005).

Recently, Okada (2006) modified the conventional SPAC method (Aki 1957) for a finite number of stations to include correlations between the circumferential stations and the central station. The SPAC coefficients in this version require calculation of a zero-order Bessel function of the first kind, and its higher even orders.

This paper reviews three methods of obtaining SPAC coefficients from a circular array: (1) the conventional, nearly continuous model (Aki 1957); (2) the discrete model for M stations (Okada 2006) and (3) the MSPAC method based on vertical microtremor components (Bettig *et al*. 2001). We then propose a new model to calculate SPAC coefficients, named the extended MSPAC (EMSPAC) method. We apply EMSPAC to the cases of discrete and nearly continuous circular arrays, with both uniform and non-uniform distributions. The resulting coefficients are compared with MSPAC coefficients. Finally, using real data from array measurements from a site in southern Tehran, we compare Rayleigh-wave dispersion curves calculated using the EMSPAC method and the MSPAC method.

2 MATHEMATICAL OVERVIEW OF METHODS FOR OBTAINING AVERAGED SPAC COEFFICIENTS

The ambient noise source is assumed to be far from the stations. We may therefore use the following representation for the vertical polarized signal at each station, in polar coordinates (r, θ) at time t (Okada 2003):

$$X(t, r, \theta) = \int_{-\infty}^{+\infty} \int_{0}^{2\pi} \exp\{i\omega t + ikr\cos(\theta - \varphi)\}\, \mathrm{d}\zeta(\omega, \varphi), \quad (1)$$

where $k = k(\omega)$ is the wavenumber. The differential amplitude $\mathrm{d}\zeta(\omega, \varphi)$ is a complex random variable, related to frequency $\mathrm{d}\omega$ and propagation direction $\mathrm{d}\varphi$ as shown in the following equation.

$$\mathrm{d}\zeta(\omega, \varphi) = \zeta(\omega + \mathrm{d}\omega, \varphi + \mathrm{d}\varphi) - \zeta(\omega, \varphi). \quad (2)$$

The SPAC function between two signals observed at a circumferential station (r, θ) and the central station $(0, \theta)$ is (Okada 2003)

$$S(r, \theta) = \mathrm{E}\left[X(t, r, \theta)\, X^*(t, 0, \theta)\right], \quad (3)$$

where E[.] is the statistical expectation and * is the complex conjugate symbol. Assuming that no coupling takes place between Rayleigh waves with different frequencies and propagation directions, the orthogonality condition implies that

$$\begin{aligned}&\mathrm{E}\left[\mathrm{d}\zeta(\omega, \varphi)\, \mathrm{d}\zeta^*(\omega', \varphi')\right] \\ &\quad = h(\omega, \varphi)\, \delta(\omega - \omega')\, \delta(\varphi - \varphi')\, \mathrm{d}\omega \mathrm{d}\varphi \mathrm{d}\omega' \mathrm{d}\varphi',\end{aligned} \quad (4)$$

where $\delta(\omega - \omega')$ is Dirac's delta function (zero when $\omega \neq \omega'$). The factor $h(\omega, \varphi)$ is the directional power spectral density (PSD) of the Rayleigh wave (Henstridge 1979), so $h(\omega, \varphi)\, \mathrm{d}\omega \mathrm{d}\varphi$ represents the average contribution to the total power received from waves with directions between φ and $\varphi + \mathrm{d}\varphi$ and having angular frequencies between ω and $\omega + \mathrm{d}\omega$. The microtremors are assumed to be wide sense stationary (WSS) and ergodic random processes, so the SPAC function is independent of the time t. Substituting (1) into (3) using (4) results in

$$S(r, \theta) = \int_{-\infty}^{+\infty} \int_{0}^{2\pi} \exp\{ikr\cos(\theta - \varphi)\}\, h(\omega, \varphi)\, \mathrm{d}\omega \mathrm{d}\varphi. \quad (5)$$

In the following subsections, we discuss two cases: nearly continuous circular arrays and M-station circular arrays.

2.1 Averaged SPAC coefficient for a nearly continuous circular array

Taking the continuous azimuthal average of eq. (5) over all circumferential stations, $\overline{S}(r) = \frac{1}{2\pi}\int_0^{2\pi} \mathrm{S}(r, \theta)\mathrm{d}\theta$, we find

$$\overline{S}(r) = \int_{-\infty}^{\infty} J_0(kr)\, h_0(\omega)\, \mathrm{d}\omega \triangleq \int_{-\infty}^{\infty} \overline{S}(r, \omega)\mathrm{d}\omega, \quad (6)$$

where $J_0(kr) = \frac{1}{2\pi}\int_0^{2\pi} \exp(ikr\cos\theta)\, \mathrm{d}\theta$ is the zero-order Bessel function of the first kind and $h_0(\omega) = \int_0^{2\pi} h(\omega, \varphi)\mathrm{d}\varphi$ is the PSD integrated over all propagation directions.

For each frequency ω, normalizing eq. (6) results in the averaged SPAC coefficient (Aki 1957).

$$\rho(\omega; r) = \overline{S}(r, \omega)/\overline{S}(0, \omega) = J_0(kr). \quad (7)$$

Once the averaged SPAC coefficient has been calculated, the phase velocities of the Rayleigh waves $c(\omega) = \omega/k(\omega)$ can be found by inverting eq. (7). This quantity is independently calculated for each frequency $f = \omega/2\pi$ after narrow-band filtering of the signals. This model is based on an imaginary circular array with a station at every possible angle, so the averaged SPAC coefficient of eq. (7) can be replaced with a more suitable one for finite arrays.

2.2 Averaged SPAC coefficient for an M-station circular array

The averaged SPAC coefficient for a uniform circular array of radius r with M circumferential stations and one station in the centre can be calculated exactly as follows (Okada 2006):

$$\rho_M(\omega; r) = J_0(kr) + 2\sum_{l=1}^{\infty} (-1)^{\nu l M} a_l J_{2\nu l M}(kr), \quad (8)$$

where $a_l = \frac{1}{h_0(\omega)}\int_0^{2\pi} \cos(2\nu l M\varphi) h(\omega, \varphi)\mathrm{d}\varphi$, $\nu = 1$ for odd M, and $\nu = 1/2$ for even M. Generally, the distribution $h(\omega, \varphi)$ is unknown in each propagation direction φ, so a closed form for a_l does not exist. However, it is evident that $-1 \leq a_l \leq 1$, and setting $a_l = 1$ in (8) leads to an upper bound for the averaged SPAC coefficient.

2.3 The MSPAC coefficient

Bettig *et al.* (2001) considered the correlations between all possible pairs of stations. They organize the pairs into a 'co-array' of several concentric rings, one ring for each interstation distance. Their method is named modified averaged SPAC (MSPAC). The MSPAC coefficient in each ring is (Bettig *et al.* 2001)

$$\begin{aligned}\rho(\omega; r_{n1}, r_{n2}) &= \frac{2}{r_{n2}^2 - r_{n1}^2}\int_{r_{n1}}^{r_{n2}} r J_0(kr)\mathrm{d}r \\ &= \frac{2}{r_{n2}^2 - r_{n1}^2}\frac{1}{k}\left[r_{n2}J_1(kr_{n2}) - r_{n1}J_1(kr_{n1})\right],\end{aligned} \quad (9)$$

where r_{n1} and $r_{n2} (r_{n1} < r_{n2})$ are the radii of the nth ring. They showed that by increasing the aperture of the array, the part of the dispersion curve that is well resolved and provides high-quality estimates of phase velocities shifts to a lower frequency band.

In the next section, we apply the idea proposed by Okada (2006) for calculating averaged SPAC coefficients to improve the MSPAC method for an M-station circular array. Then we will show that in a nearly continuous circular array, the MSPAC coefficient (9) requires correction; a different weighting function is needed to combine the co-array rings in this case.

3 EMSPAC COEFFICIENTS FOR THE CIRCULAR ARRAY

3.1 Uniform discrete model

In this section, we calculate the MSPAC coefficient for each pair of stations in a finite, uniform circular array. In an M-station array, the number of unique pairs, not including the central station, is $M(M - 1)/2$. Each possible interstation distance is mapped to a circle of equivalent radius, and the set of such circles is called the co-array. For odd M, the number of stations on each circle of the co-array is equal to M. For even M, each circle except for the outermost has M stations and the outermost has $M/2$ stations. The total number of circles in the co-array is $(M-1)/2$ for odd M and $M/2$ for even M. Thus, the number of circles in the co-array can be written as $\lfloor M/2 \rfloor$, meaning the biggest integer smaller than or equal to $M/2$. One can readily see that the radius of each circle in the co-array is $r_j = 2r\sin(\frac{j\pi}{M})$, $j = 1, 2, \ldots, \lfloor M/2 \rfloor$. Hence, using eq. (8), the EMSPAC coefficient for the jth circle is

$$\rho_M(\omega; r, j) = J_0\left(2kr\sin\left(\frac{j\pi}{M}\right)\right) + 2\sum_{l=1}^{\infty}(-1)^{\nu l M_j} \times a_l J_{2\nu l M_j}\left(2kr\sin\left(\frac{j\pi}{M}\right)\right), \quad j = 1, 2, \ldots, \lfloor M/2 \rfloor, \tag{10}$$

where M_j is the number of stations on the jth circle.

The EMSPAC coefficient in eq. (10) is comparable to the MSPAC coefficient in eq. (9) when $r_{n2} \to r_{n1}$, for each n. On the other hand, if $r_{n2} \to r_{n1}$ in (9), it is easy to show that $\lim_{r_{n2}\to r_{n1}} \rho(\omega; r_{n1}, r_{n2}) = J_0(kr_{n1})$, which is exactly the same as the conventional averaged SPAC coefficient. Therefore, in the case $\Delta r_n = r_{n2} - r_{n1} = 0$, the MSPAC method is equivalent to the conventional SPAC method.

In a uniform circular M-station array, the only difference between the SPAC coefficients calculated in eqs. (10) and (9) is the second term on the right-hand side of eq. (10). Fig. 1 depicts the two SPAC coefficients for $M = 5$ and $j = 1, 2$. In the region of interest (below the aliasing limit) the models fit well, which is also visible in the real data results in Fig. 7. It is obvious that the error introduced by using the nearly continuous model (a zero-order Bessel function of the first kind) increases for larger rings.

On the other hand, the spatial sampling of an M-station circular array determines the Nyquist wavenumber for that array, which in SPAC processing is the maximum wavenumber beyond which aliasing error occurs. For a circle array, increasing M decreases the aliasing error. For fixed M, increasing the radius of the array increases the aliasing effect.

3.2 Non-uniform discrete model

In a non-uniform, M-station circular array, stations may be placed at any position on the circumference. Therefore, relation (8) cannot be used. Instead, we use the Jacobi–Anger expansion (Arfken & Weber 2001).

$$\exp\{ikr\cos(\theta - \varphi)\} = J_0(kr) + 2\sum_{n=1}^{\infty} i^n J_n(kr)\cos\{n(\theta - \varphi)\}. \tag{11}$$

Substituting this form into eq. (5), we obtain

$$S(r, \theta) = \int_{-\infty}^{+\infty}\left(J_0(kr)h_0(\omega) + 2\sum_{n=1}^{\infty} i^n J_n(kr)\int_0^{2\pi}\cos\{n(\theta - \varphi)\}\, h(\omega, \varphi)\mathrm{d}\varphi\right)\mathrm{d}\omega. \tag{12}$$

The azimuthal average is then defined as $\overline{S}(r) = \frac{1}{2\pi}\sum_{l=1}^{M} S(r, \theta_l)\Delta\theta_l$, where $\Delta\theta_l$ is the azimuthal difference between stations l and $(l+1)$; $\Delta\theta_l = \theta_{l+1} - \theta_l$, $l = 1, 2, 3, \ldots, M$

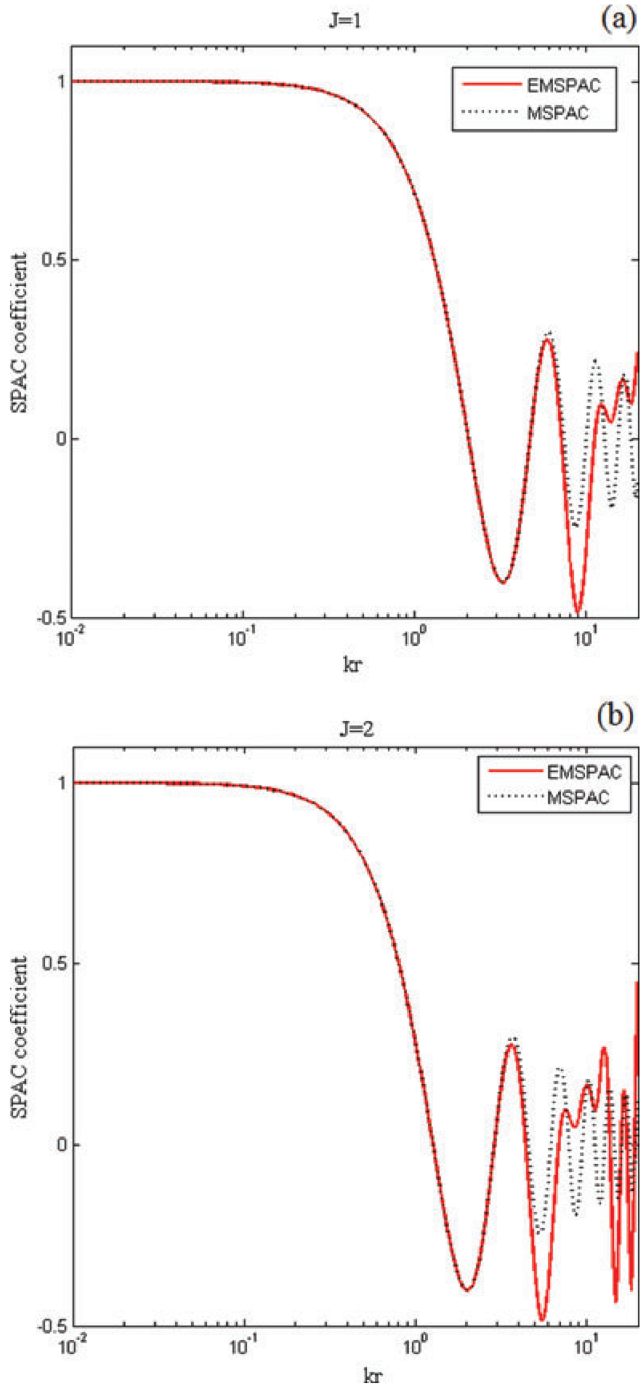

Figure 1. Comparing EMSPAC and MSPAC coefficients for $M = 5$ for two different circles in the co-array, M is the number of stations and j is the number of the circle in the co-array. (a) Comparing the coefficients in the first circle, $j = 1$. (b) Comparing the coefficients in the second circle, $j = 2$.

and $\theta_1 = 0$. Therefore,

$$\overline{S}(r) = \int_{-\infty}^{+\infty}\left(J_0(kr)h_0(\omega) + 2\sum_{n=1}^{\infty} i^n J_n(kr) \times \int_0^{2\pi}\left[\sum_{l=1}^{M}\cos\{n(\theta_l - \varphi)\}\Delta\theta_l\right]h(\omega, \varphi)\mathrm{d}\varphi\right)\mathrm{d}\omega \triangleq \int_{-\infty}^{\infty}\overline{S}(r, \omega)\mathrm{d}\omega. \tag{13}$$

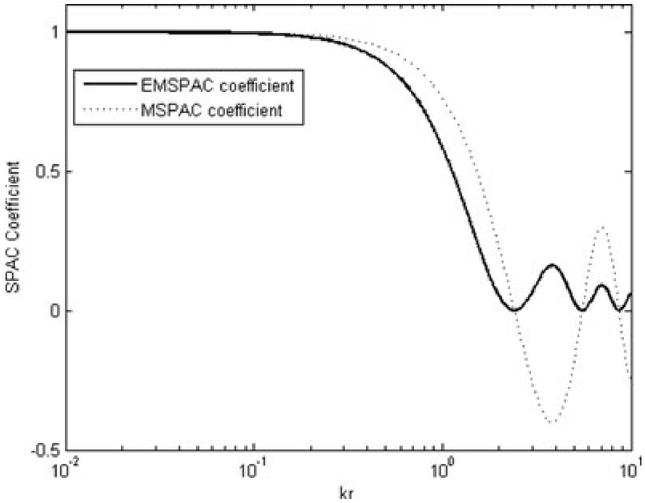

Figure 2. Comparing EMSPAC coefficients from relation (21) with MSPAC coefficients from relation $J_1(2kr)/kr$ for nearly continuous circular array.

Finally, the averaged SPAC coefficient for a non-uniform M-station circular array is obtained by normalizing (13). The result is

$$\rho_M(\omega; r) \stackrel{\Delta}{=} \overline{S}(r, \omega)/\overline{S}(0, \omega) = J_0(kr) + \frac{2}{h_0(\omega)} \sum_{n=1}^{\infty} (-1)^n J_{2n}(kr) \times \int_0^{2\pi} \left[\sum_{l=1}^{M} \cos\{2n(\theta_l - \varphi)\} \Delta\theta_l \right] h(\omega, \varphi) \, d\varphi. \quad (14)$$

Here n has been replaced by $2n$ to make the averaged SPAC coefficient a real quantity. This relation reduces to eq. (8) for a uniform circular array if $\Delta\theta_l = \frac{2\pi}{M}$, according to definition a_l and the equality $\sum_{l=1}^{M} \cos\{2n(\theta_l - \varphi)\} = M\cos\{2\nu p M(\theta_1 - \varphi)\}\, \delta_{n,\nu pM}$, where $p = 1, 2, 3, \ldots$ Note that $\nu = 1$ for odd M, and $\nu = 1/2$ for even M. We can also use eq. (14) to deduce the EMSPAC coefficient for the jth circle with radius r_j.

$$\rho_M(\omega; r_j) = J_0(kr_j) + \frac{2}{h_0(\omega)} \sum_{n=1}^{\infty} (-1)^n J_{2n}(kr_j) \times \int_0^{2\pi} \left[\sum_{l=1}^{M_j} \cos\{2n(\theta_l - \varphi)\} \Delta\theta_l \right] h(\omega, \varphi) d\varphi, \quad (15)$$

where M_j is the number of stations on the jth circle.

Eq. 15 takes into account non-uniform discrete arrays, but as the propagation direction must be known, it can only be used in practice when there is, for example, one dominant propagation direction known for instance from F–K analysis.

3.3 Nearly continuous model

It is clear that increasing the number of circumferential stations makes the circles in the co-array closer together. Hence, for a nearly continuous array, the radii of the circles in the co-array cover the entire interval from zero to $2r$. In this case, the SPAC coefficient is

$$\rho(\omega; r) = \frac{2}{\pi} \int_0^{\pi/2} J_0(2kr \sin\alpha) \, d\alpha. \quad (16)$$

To arrive at eq. (16), first we calculate the MSPAC coefficient for an arbitrary ring whose radius is between x and $x + dx$. The contribution of this thin ring to the MSPAC coefficient is represented by a weighting function $w(x)$. The MSPAC coefficient is obtained

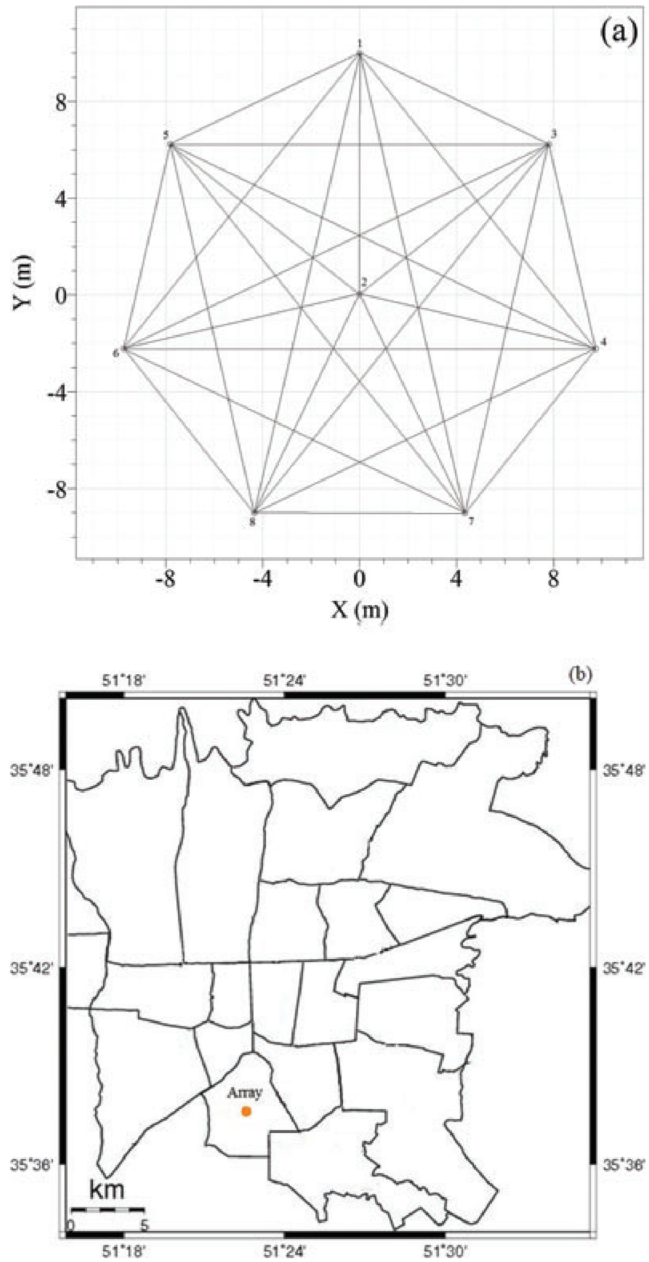

Figure 3. (a) Array configuration of the field experiment in southern Tehran. (b) Location of the array in the map of Tehran.

by summing the influence of all such rings between 0 and $2r$.

$$\rho(\omega; r) = \int_0^{2r} J_0(kx) \, w(x) dx \,. \quad (17)$$

The following approach is used to find $w(x)$. In a discrete model, the radius of the jth circle of the co-array is $r_j = 2r \sin(\frac{j\pi}{M})$. The formula $j = \frac{M}{\pi} \sin^{-1}(\frac{r_j}{2r})$ therefore gives the label of each circle. To derive the nearly continuous model from the discrete model, define the number of circles between x and $x + dx$ as

$$F(x) \, dx = \frac{M}{\pi} \sin^{-1}\left(\frac{x + dx}{2r}\right) - \frac{M}{\pi} \sin^{-1}\left(\frac{x}{2r}\right). \quad (18)$$

Approximating the terms on the right-hand side by linear Taylor series in dx, we find

$$F(x) \, dx = \frac{M}{\pi} \frac{dx}{\sqrt{1 - (x/2r)^2}}. \quad (19)$$

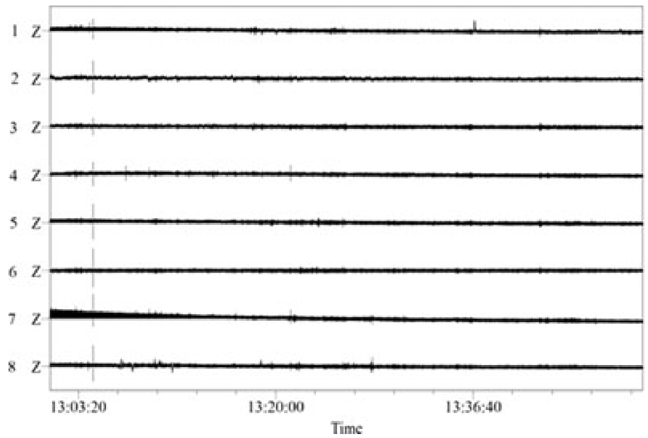

Figure 4. Near one hour simultaneous microtremor records on the vertical components at seven stations placed on a circumference with radius of 10 m, and one in the centre.

Thus, $w(x)\,\mathrm{d}x$ is just the normalized form of $F(x)\,\mathrm{d}x$.

$$w\,(x) = \frac{1}{\pi r}\frac{1}{\sqrt{1-(x/2r)^2}}. \tag{20}$$

Substituting (20) into (17) yields

$$\rho\,(\omega; r) = \frac{1}{\pi \mathrm{r}}\int_0^{2r}\frac{\mathrm{J}_0\,(kx)}{\sqrt{1-(x/2r)^2}}\,\mathrm{d}x\,. \tag{21}$$

If x is replaced with $2r\sin\alpha$, (21) is equal to (16). There is no closed form solution for integrals (16) or (21).

Letting $r_{n1} \to 0$ and $r_{n2} \to 2r$, the right-hand side of eq. (9) changes to $\rho(\omega; 0, 2r) = J_1\,(2kr)\,/\,kr$. This result is different from that obtained by setting r to the same values in eq. (21). The extent of the difference is depicted in Fig. 2. In fact, the major difference between these two models is the weighting density function $w(x)$ introduced in eq. (20).

We now introduce an important inequality; in Figs 1 and 2 it can be seen that

$$x|_{\rho(x)=a} < x|_{J_0(x)=a}, \quad \text{for} \min_{x:\rho'(x)=0} \rho(x) \le a \le 1. \tag{22}$$

Relation (22) indicates that the coefficients obtained by the EMSPAC method are shifted to lower wavenumbers (i.e. longer wavelengths at fixed r) compared to the conventional MSPAC model.

4 REAL DATA

We conducted measurements using a uniform circular array of seven stations and one station in the centre. The array was composed of Guralp CMG6TD seismic stations (Fig. 3a), and its aperture was near 20 metres. Ambient noise measurements were performed in 2007 at a site in the south of Tehran (Fig. 3b). Fig. 4 illustrates the data with a sample of simultaneous microtremor records (vertical components) taken at the seven stations.

After applying a bandpass filter to the records, we calculated the averaged SPAC coefficients of the vertical wavefield. The SPAC coefficients are computed for pairs with similar interstation distances by limiting the data to a narrow frequency band and ‘ring radius’. Fig. 5 plots the azimuths and interstation distances for the array; each dot represents one pair of stations. Fig. 6 shows the averaged SPAC coefficient calculated in each ring of the co-array.

The averaged SPAC coefficients deduced in each ring are then used in eqs (9) and (10) to deduce the dispersion curves. Fig. 7 compares the dispersion curves of all rings calculated using the real data field in the EMSPAC and MSPAC methods.

5 DISCUSSION AND CONCLUSION

This paper has presented an extension of the MSPAC technique for discrete and nearly continuous circular arrays. The proposed model considers all possible station pairs in the array by defining a co-array consisting of concentric virtual arrays representing pairs of stations separated by equal distances (or similar distances in the case of non-uniform arrays).

The EMSPAC coefficients obtained for discrete and nearly continuous arrays are displayed theoretically in Figs 1 and 2, and compared with those obtained by the MSPAC method. Compared to MSPAC, for the nearly continuous case the peak resolution of the EMSPAC method occurs at lower wavenumbers (longer wavelengths) since the slope of its averaged SPAC coefficient with respect to wavenumber is steeper. We also demonstrated that the averaged conventional SPAC coefficient is a special case of our proposed

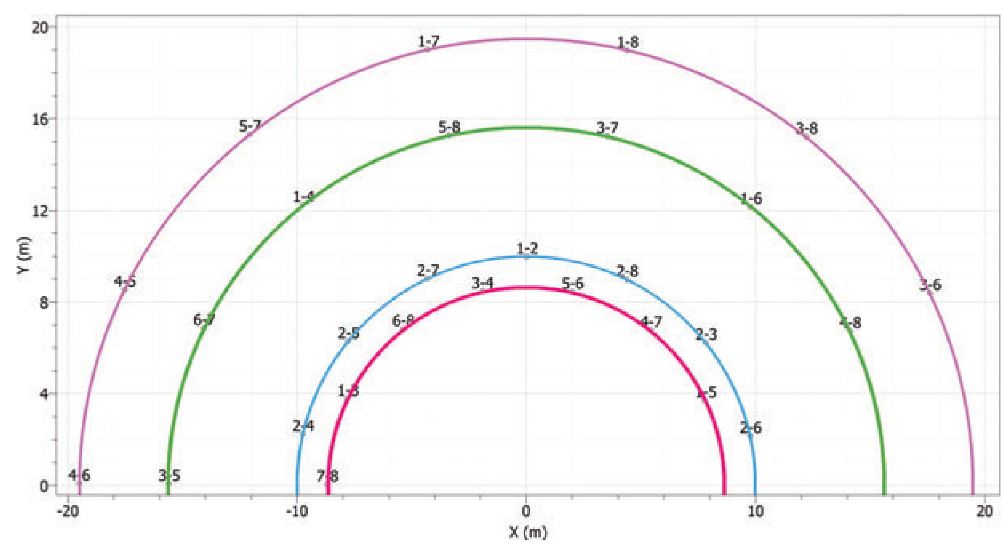

Figure 5. Azimuth–interdistance plot for the array; each dot represents one couple of stations, all dots are divided in four rings.

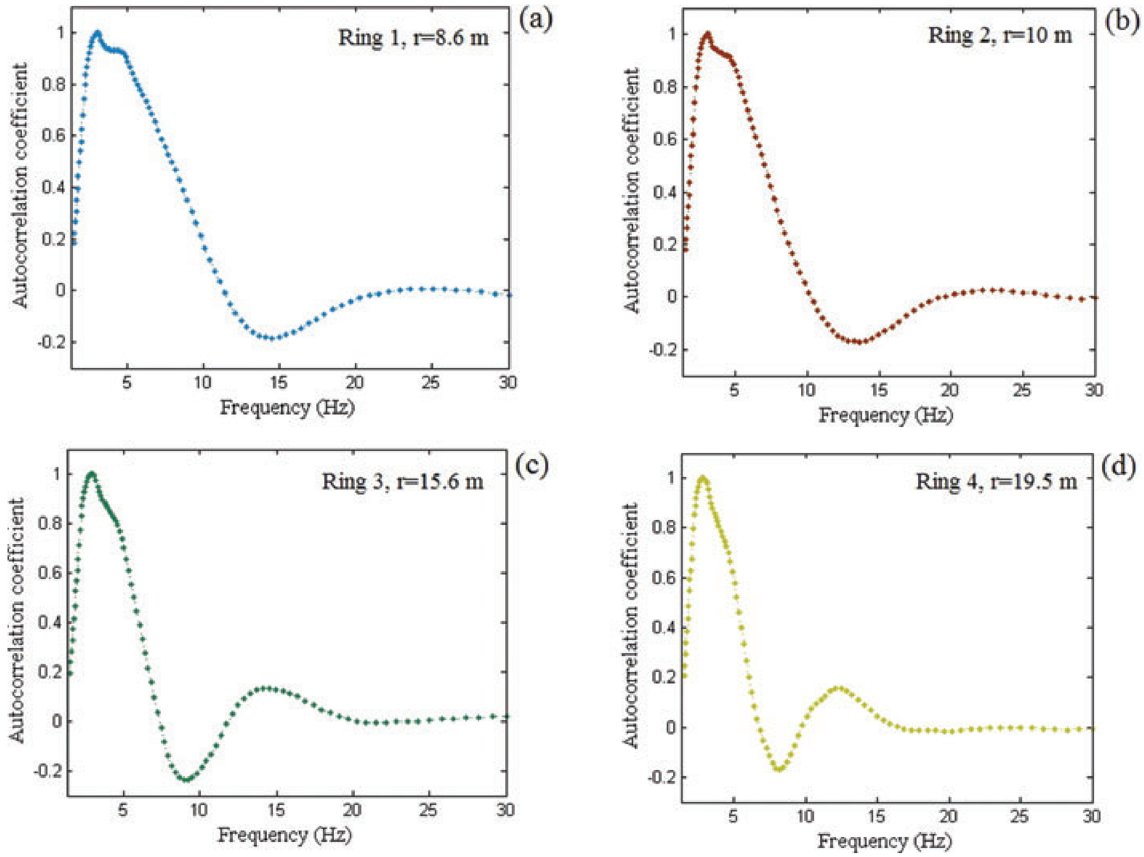

Figure 6. Averaged SPAC coefficients obtained in four rings using real field data.

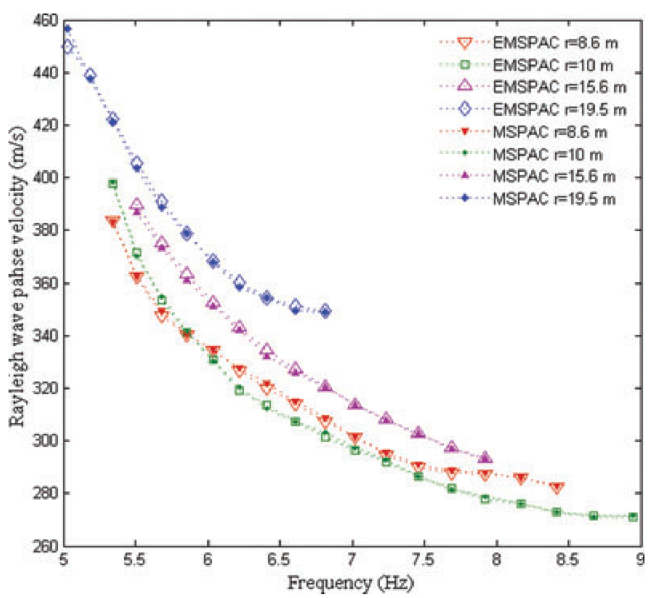

Figure 7. Comparing deduced dispersion curves in MSPAC and EMSPAC methods using real field data in four rings with radii 8.6 m, 10 m, 15.6 m and 19.5 m.

model. The major difference between the MSPAC and EMSPAC models is the weighting density function $w(x)$ used to integrate rings in the co-array. This difference prevents our model from being considered a special case of the MSPAC model.

The discrete EMSPAC and MSPAC formulae are also tested against real data obtained by a 7-station circular array, which results in four averaged SPAC coefficients for the four rings in the co-array. Substituting the averaged SPAC coefficients for each frequency into the left-hand side of relation (10), we obtained Rayleigh-wave dispersion curves for both methods. Where, considering only the first term in the right-hand side of relation (10), $J_0(2kr\sin(\frac{i\pi}{M}))$, holds for MSPAC method and taking into account all terms it holds for EMSPAC method. The results are compared in Fig. 7 for all rings. For each frequency, the Rayleigh-wave phase velocities deduced in MSPAC and EMSPAC methods are very similar. This is also obvious when looking at Fig. 1, for the selected frequency bandwidths that avoid the aliasing effects. It seems that the small differences between deduced dispersion curves in Fig. 7 are due to the resolution in the inversion process.

ACKNOWLEDGMENTS

The authors gratefully thank the Editor, Prof. Xiaofei Chen and the anonymous referee for the constructive comments, which significantly improved this article. This research was supported by University of Tehran grant no. 6201025-1-02. We are also grateful to the International Institute of Earthquake Engineering and Seismology (IIEES) that allowed using the data of project no. 6506.

REFERENCES

Aki, K., 1957. Space and time spectra of stationary stochastic waves, with special reference to microtremors, *Bull. Earthq. Res. Inst.,* **35,** 415–456.

Apostolidis, P., Raptakis, D., Roumelioti, Z. & Pitilakis, K., 2004. Determination of S-wave velocity structure using microtremors and SPAC method applied in Thessaloniki (Greece), *Soil Dyn. Earthq. Eng.,* **24,** 49–67.

Arfken, G.B. & Weber, H.J., 2001. *Mathematical Methods for Physicists,* 5th edn, Harcourt Academic Press, San Diego.

Asten, M.W., 1976. The use of microseisms in geophysical exploration, *PhD thesis,* Macquarie University, Australia.

Bettig, B., Bard, P.Y., Scherbaum, F., Riepl, J., Cotton, F., Cornou, C. & Hatzfeld, D., 2001. Analysis of dense array noise measurements using the modified spatial autocorrelation method (SPAC): application to the Grenoble area, *Boll. Geofis. Teor. Appl.,* **42,** 281–304.

Capon, J., 1969. High-resolution frequency-wavenumber spectrum analysis, *Proceedings IEEE,* **57,** 1408–1418.

Chávez-García, F.J. & Luzón, F., 2005. On the correlation of the seismic microtremors, *J. geophys. Res.,* **110**. doi:10.1029/2005JB003671.

Chávez-García, F.J., Rodríguez, M. & Stephenson, W.R., 2005. An alternative approach to the SPAC analysis of microtremors: exploiting stationarity of noise, *Bull. seism. Soc. Am.,* **95,** 277–293.

Cho, I., Tada, T. & Shinozaki, Y., 2006. A generic formulation for microtremor exploration methods using three-component records from a circular array, *Geophys. J. Int.,* **165**(1), 236–259.

García-Jerez, A., Luzón, F. & Navarro, M., 2006. Computation of dispersion curves for Rayleigh and Love waves using horizontal components of seismic microtremor, in *Proceedings of the 8th U.S. National Conference on Earthquake Engineering,* San Francisco, USA, April 2006, Paper No. 1377.

García-Jerez, A., Luzón, F., Navarro, M. & Pérez-Ruiz, J.A., 2008. Determination of elastic properties of shallow sedimentary deposits applying a spatial autocorrelation method, *Geomorphology,* **93,** 74–88.

Henstridge, J.D., 1979. A signal processing method for circular arrays, *Geophysics,* **44,** 179–184.

Kudo, K. *et al.*, 2002. Site specific issues for strong ground motions during the Kocaeli, Turkey Earthquake of August 17, 1999, as inferred from array observations of microtremors and aftershocks, *Bull. seism. Soc. Am.,* **92,** 448–465.

Lacoss, R.T., Kelly, E.J. & Toksoz, M.N., 1969. Estimation of seismic noise structure using arrays, *Geophysics,* **34,** 21–38.

Matsuoka, T., Umezawa, N. & Makishima, H., 1996. Experimental studies on the applicability of the spatial autocorrelation method for estimation of geological structures using microtremors, *Butsuri Tansa,* **49,** 26–41.

Morikawa, H., Sawada, S. & Akamatsu, J., 2004. A method to estimate phase velocities of Rayleigh waves using microseism simultaneously observed at two sites, *Bull. seism. Soc. Am.,* **94,** 961–976.

Ohori, M., Nobata, A. & Wakamatsu, K., 2002. A comparison of ESAC and FK methods of estimating phase velocity using arbitrarily shaped microtremor arrays, *Bull. seism. Soc. Am.,* **92**(6), 2323–2332.

Okada, H., 2003. The Microtremor Survey Method (translated by Koya Suto), *Geophysical Monograph Series,* No.12, Society of Exploration Geophysicists.

Okada, H., 2006. Theory of efficient array observations of microtremors with special reference to the SPAC method, *Explor. geophys.,* **37,** 73–85.

Okada, H., Matsushima, T., Moriya, T. & Sasatani, T., 1990. An exploration technique using long-period microtremors for determination of deep geological structures under urbanized areas, *Butsuri Tansa,* **43,** 402–417.